Novel finite-differencing techniques for numerical relativity: application to black hole excision

Gioel Calabrese[1], Luis Lehner[1], David Neilsen[1], Jorge Pullin[1], Oscar Reula[2], Olivier Sarbach[1], and Manuel Tiglio[1]
1 *Department of Physics and Astronomy, Louisiana State University, 202 Nicholson Hall, Baton Rouge, LA 70803-4001*
2 *FaMAF, Universidad Nacional de Cordoba, Cordoba, Argentina 5000*

We use rigorous techniques from numerical analysis of hyperbolic equations in bounded domains to construct stable finite-difference schemes for Numerical Relativity, in particular for their use in black hole excision. As an application, we present 3D simulations of a scalar field propagating in a Schwarzschild black hole background.

arXiv:gr-qc/0302072v1 18 Feb 2003

The numerical implementation of Einstein's equations represents a daunting task. The involved nature of the equations themselves, and a number of technical difficulties (related to the necessarily finite computational domain, the limitations in relative computational power and the need to deal with singularities, constraints and gauge freedom) imply a significant challenge.

Numerical solutions of Einstein's equations involve solving a nonlinear set of partial differential equations on a bounded domain, and formally constitute an initial-boundary-value problem (IBVP). Constructing stable and long term well behaved numerical approximations for such systems with boundaries is highly non-trivial. Here the term numerical stability is used in the sense that is equivalent, through Lax's theorem, to convergence (that is, the property that the numerical solution will approach the continuum one when resolution is increased). Delicate complications arise due to corner and edges at outer (and possible inner) boundaries, all of which introduce subtleties for a stable implementation.

Recently, however, several sophisticated tools of rigorous numerical analysis have been developed for systematically constructing stable numerical schemes for IBVP's. They employ a discrete form of well-posedness and thus are stable by construction, at least for linear systems. At this time, these tools have essentially not been used by the numerical relativity community. The purpose of this paper is to outline their use, in particular for black hole excision.

An IBVP consists of three ingredients: a partial differential equation, initial and boundary data. It is well-posed if a solution exists, is unique, and depends continuously on the initial and boundary data. It is well known that stable finite difference schemes approximating an IBVP can only be constructed for well-posed systems. While problems in general relativity are typically nonlinear we consider here the linear IBVP, as stability in the linearized case is a necessary condition for stability in the full nonlinear system and these methods may also be applied to nonlinear equations. Consider the linear IBVP on a domain $[0,\infty)\times\Omega$

$$\partial_t u = A(t,\vec{x})^i\partial_i u + B(t,\vec{x})u, \quad (1)$$

$$u(0,\vec{x}) = f(\vec{x}), \quad (2)$$

$$w_+(t,\vec{x}) = Sw_-(t,\vec{x}) + g(t,\vec{x})\ ,\vec{x}\in\partial\Omega, \quad (3)$$

where u is a vector-valued function, w_+ and w_- are incoming and outgoing modes, and S is sufficiently small (maximally dissipative boundary conditions [3]). The system is assumed to be symmetric hyperbolic, i.e., there exists a symmetric positive definite matrix $H(t,\vec{x})$, the symmetrizer, satisfying $HA^i = (HA^i)^T$. The usual proof of well-posedness proceeds by defining an "energy", $\mathcal{E} = \int_\Omega u^T H u\, d^3x$, and by showing that $\mathcal{E}$ can be bounded as a function of the initial and boundary data. Analogously, a way to construct stable numerical schemes is to design them such that energy estimates hold at the discrete level [2]. This is the procedure we shall follow in this paper.

Our construction involves four steps. (1) We construct discrete derivative operators and a scalar product so that a semi-discrete energy estimate holds. The spatial derivatives are then discretized using these operators, resulting in a semi-discrete system of ordinary differential equations. (2) We impose boundary conditions in a way that does not spoil the previous semi-discrete energy estimate. In particular, we account for effects of boundary edges and vertices. Steps (1) and (2) guarantee numerical stability of the semi-discrete system. (3) We may add artificial dissipation and/or arrange the spatial discretization to achieve optimal energy bounds. (4) Finally, an appropriate time integrator is chosen so that *fully discrete stability* holds.

Step (1): The equations are discretized on a domain Ω with an inner boundary to accommodate for black hole excision. While several grid geometries are possible, we concentrate on the simplest case of a cubical domain from which an inner, smaller cube has been removed (both cubes aligned with the grid). We introduce the grid points $\vec{r}_{ijk} = (i\Delta x, j\Delta y, k\Delta z)\in\Omega$ and assume that some of these points lie on the boundary $\partial\Omega$. A scalar product, Σ, between any two real vector-valued grid functions u and v, is defined as

$$(u,v)_\Sigma = \Delta x\Delta y\Delta z \sum_{i,j,k=0}^{N} \sigma_{ijk} u^T_{ijk} v_{ijk}, \quad (4)$$

where σ_{ijk} are defined below and in the sum $\vec{r}_{ijk}\in\Omega$. A semi-discrete energy is then defined by $E = (u, Hu)_\Sigma$.

A key ingredient for deriving the continuum energy estimate is integration by parts. Similarly, in order to get a semi-discrete energy estimate, one must construct the

difference operators, D, and Σ in such a way that the discrete version of integration by parts, called *summation by parts* (SBP), holds. In one dimension, SBP is expressed by $(u, Dv)_\Sigma + (Du, v)_\Sigma = u_N v_N - u_0 v_0$, and this definition can be generalized to higher dimensions and more complicated domains.

A detailed calculation shows that SBP for our chosen Ω holds by defining (similar definitions for y, z directions)

$$D^{(x)} = \begin{cases} D^{(x)}_{\pm} u_{ijk} & \text{at } x = \text{const. faces,} \\ & x = \text{const. OB edges} \\ & \text{and OB vertices} \\ \left(\frac{1}{3} D^{(x)}_{\pm} + \frac{2}{3} D^{(x)}_0\right) u_{ijk} & \text{at } x = \text{const. IB edges} \\ \left(\frac{1}{7} D^{(x)}_{\pm} + \frac{6}{7} D^{(x)}_0\right) u_{ijk} & \text{at IB vertices} \\ D^{(x)}_0 u_{ijk} & \text{everywhere else} \end{cases}$$

where IB and OB stand for inner and outer boundary respectively, $D^{(x)}_+ u_{ijk} = (u_{i+1\,jk} - u_{ijk})/\Delta x$, $D^{(x)}_- u_{ijk} = (u_{ijk} - u_{i-1\,jk})/\Delta x$ and $D^{(x)}_0 u_{ijk} = (u_{i+1\,jk} - u_{i-1\,jk})/(2\Delta x)$. The $\pm$ signs indicate whether non-excised points are to the right or left, respectively, of the boundary point. The weights σ_{ijk} in (4) are defined to be 1 in the interior, 1/2 at the faces of IB and OB, 1/4 at the edges of OB, 3/4 at the edges of IB, 1/8 at the vertices of OB, 7/8 at the vertices of IB, and zero in the excised region. This difference operator is second-order accurate at the interior and first-order at boundaries, yielding in principle, a scheme with overall second-order accuracy[4].

Step (2): In contrast to the continuum problem, an examination of boundary terms left after SBP in the energy estimate indicates that edge and vertex boundary points make a finite contribution to E at fixed resolution. These contributions show precisely how to impose boundary conditions at these points. They have to be imposed on incoming characteristic modes defined by some "effective" normal vectors n. For instance, on a *uniform* grid ($\Delta x = \Delta y = \Delta z$), at an edge one has $n = (n_a + n_b)/\sqrt{2}$, and at a vertex $n = (n_a + n_b + n_c)/\sqrt{3}$ (where n_a, n_b and n_c are unit vectors of the intersecting faces). Boundary conditions along these effective directions have to be imposed without destroying the semi-discrete energy estimate. Following Olsson [5], we do so by projecting the right hand side (RHS) of the evolution equations at boundary points onto the subspace of the grid functions that satisfy the discretized boundary conditions. The projection is by construction self-adjoint with respect to Σ, which ensures that the solution of the projected semi-discrete system will satisfy the boundary conditions without compromising numerical stability.

Step (3): At a fixed resolution, even convergent codes may generate significant error growth as time progresses, and it is often desirable to minimize this growth. This may be achieved by adding artificial dissipation, by rearranging the semi-discrete equations in a specific manner to obtain optimal estimates, or by doing both. We briefly summarize these two procedures.

In numerical simulations a dissipative term, $(Q^{(x)}_d + Q^{(y)}_d + Q^{(z)}_d)u$, is sometimes added to the RHS of Eq. (1), which damps high frequency modes but does not affect the accuracy of the scheme. Requiring $(u, Q^{(x)}_d u)_\Sigma \le 0$ ensures that the semi-discrete energy estimate still holds. We have modified the Kreiss–Oliger dissipation operator for our black hole excision geometry and Σ. This modified operator has the standard form on the grid interior (shown here for the x direction)

$$Q^{(x)}_d u_{ijk} \;=\; -\epsilon \Delta x^3 (D^{(x)}_+ D^{(x)}_-)^2 u_{ijk},$$

(where ϵ is a parameter satisfying $\epsilon \ge 0$.) However, it is modified near boundaries to satisfy $(u, Q^{(x)}_d u)_\Sigma \le 0$. Let (i_0, j, k) label a point on a $x =$ constant boundary with neighbors $(i_0 - 1, j, k)$ and $(i_0 + 1, j, k)$. Near this boundary point $Q^{(x)}_d$ becomes

$$\begin{aligned} Q^{(x)}_d u_{i_0 - 1} &= -\epsilon \Delta x (D^{(x)2}_- - 2 D^{(x)}_+ D^{(x)}_-) u_{i_0 - 1}, \\ Q^{(x)}_d u_{i_0} &= -\frac{\epsilon \Delta x}{\sigma_{i_0}} (\sigma_{i_0 - 1} D^{(x)2}_- + \sigma_{i_0 + 1} D^{(x)2}_+) u_{i_0}, \\ Q^{(x)}_d u_{i_0 + 1} &= -\epsilon \Delta x (D^{(x)2}_+ - 2 D^{(x)}_+ D^{(x)}_-) u_{i_0 + 1}, \end{aligned}$$

where the indices jk are suppressed for clarity, and $Q^{(x)}_d$ is set to zero for points outside the domain.

A second method for controlling unnecessary growth is by rearranging the discretized equations so the optimal estimates for the continuum hold at the semi-discrete level. For instance, if at the continuum the system exhibits energy conservation, it is important to preserve it at the semi-discrete level. For example, assuming that Eq. (1) has time-independent coefficients and that $\partial_i (H A^i) = H B + (H B)^T$, $\mathcal{E}$ is conserved if appropriate boundary conditions are given. The solution of $\partial_t u = A^i(x) D_i u + B(x) u$ may yield growth in E, due to the lack of a Leibniz rule at the discrete level. However, one can show that rearranging the semi-discrete RHS of (1) as

$$\frac{1}{2} A^i D_i u + \frac{1}{2} H^{-1} D_i (H A^i u) + \left(B - \frac{1}{2} H^{-1} \partial_i (H A^i) \right) u,$$

gives a non-increasing E, and therefore the discrete solution will not grow. This idea is closely related to the concept of *strict stability* [5].

Step (4): Finally, stability of the fully discrete system follows if it is integrated with a scheme that satisfies the (necessary and sufficient) *local stability* condition or the (sufficient) preservation of energy estimate's condition (e.g., third or fourth order Runge–Kutta [6]).

An example: Wave propagation on a black hole spacetime $g_{\mu\nu}$ presents some of the same challenges as the full Einstein equations (e.g. constraint preservation, boundary conditions, excision of the singularity). Thus it is an ideal test bed to demonstrate the techniques described in this paper. We write the wave equation in first-order form,

$$\nabla_\mu \Phi = V_\mu \;, \quad \nabla^\mu V_\mu = 0 \;, \quad \nabla_\mu V_\nu = \nabla_\nu V_\mu \;, \qquad (5)$$

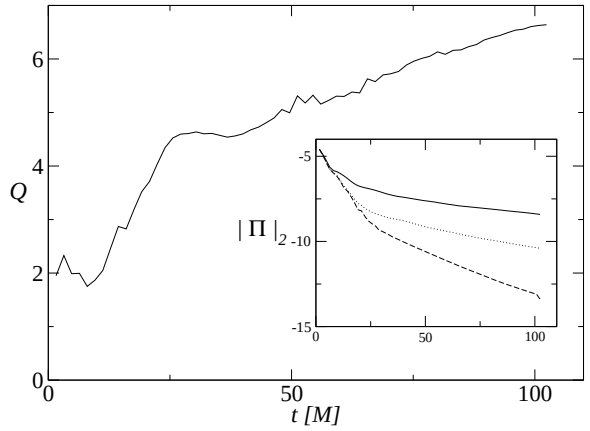


FIG. 1: The self-convergence factor, Q, as a function of time, where $Q \equiv \log_2(||f_{\Delta x} - f_{2\Delta x}||/||f_{2\Delta x} - f_{4\Delta x}||)$, and $f_{\Delta x}$, $f_{2\Delta x}$, and $f_{4\Delta x}$ represent numerical solutions calculated on uniform grids with corresponding gridspacing. The inset shows the L_2 norm of the variable Π vs. time for the three resolutions. The solution is calculated on the domain $x^i \in [1.5M, 5.5M]$, using 41^3, 81^3 and 161^3 grid points, dissipation parameter $\epsilon = 0$, and Courant factor $\lambda = 0.8$. Since we are outside the hole, we chose $b^i = 0$, giving a symmetric hyperbolic formulation. Π has non-zero initial data of compact support, and all other fields are initially set to zero. The solution is essentially second order convergent until it decreases several orders of magnitude. After that the self-convergence factor grows and the evolution is followed roughly until the solution for the finest resolution reaches truncation error (about 25 crossing times).

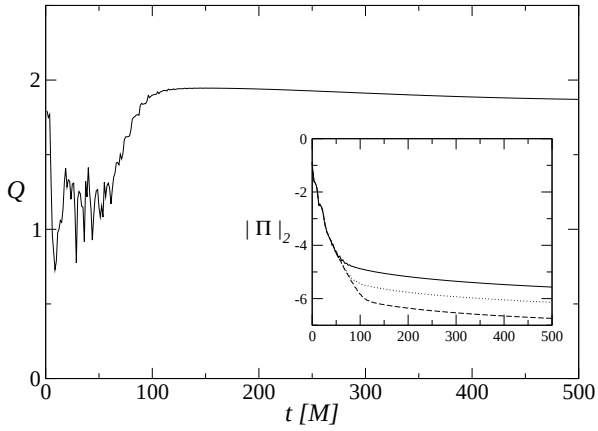


FIG. 2: This figure shows the self-convergence factor defined in Fig. 1, Q. A non-trivial b^i smoothly interpolating is used so that the system is everywhere symmetric hyperbolic. The domain is $x, y, z \in [-4M, 4M]$, with an excised region $x, y, z \in [-0.375M, 0.375M]$. The Courant factor and dissipation are $\lambda = 1$, $\epsilon = 0.02$, respectively, and runs with 65^3, 129^3 and 257^3 grid points are used to calculate Q. The initial part of the plot shows lower than second order convergence. However, experiments in one dimension show a similar effect for comparable grid spacings; though the convergence factor asymptotically approaches two as resolutions are increased.

with ∇_μ the covariant derivative. To split these equations into evolution equations and constraints, we specify a future-directed time-like vector u^μ, and contract the first and the last equation with it. The evolution equations are

$$\pounds_u \Phi = u^\mu V_\mu \equiv \Pi, \quad \nabla^\mu V_\mu = 0, \quad \pounds_u V_\mu = \nabla_\mu \Pi, \qquad (6)$$

where $\pounds_u$ is the Lie derivative with respect to u^μ. This system is symmetric hyperbolic. Due to the evolution equations, the constraints $C_\mu \equiv V_\mu - \partial_\mu \Phi = 0$, $C_{\mu\nu} \equiv \nabla_\mu V_\nu - \nabla_\nu V_\mu = 0$ are Lie-dragged by u^μ, i.e., $\pounds_u C_\mu = 0$, $\pounds_u C_{\mu\nu} = 0$.

Although the discussion below applies to any background geometry, for definiteness we specialize to the Schwarzschild background. This spacetime possesses a time-like Killing field, $k^\mu = (\partial_t)^\mu$, and the future directed unit normal n^μ to the $t =$ const. slices is given by $(k^\mu - \beta^\mu)/\alpha$. We denote with α, β^i and h_{ij} the lapse, shift and three-metric, respectively. A natural choice for the vector field u^μ is n^μ, however this requires care specifying boundary data compatible with the constraints. For a particular coupling between the in- and out-going modes, we have found maximally dissipative boundary conditions compatible with the constraints. Unfortunately, they imply reflective boundary conditions in the sense that (for homogeneous boundary data and in the absence of inner boundaries) the physical energy of the scalar field Φ is exactly conserved. Choosing a different formulation with $u^\mu = k^\mu$ allows us to impose radiative boundary conditions, in the sense that the physical energy decreases when the wave reaches the boundary. In this formulation the constraint variables C_μ and $C_{\mu\nu}$ propagate tangentially to the boundaries, and thus the constraints are automatically satisfied when satisfied initially. Moreover, this formulation has the advantage that its symmetrizer agrees with the physical energy. Unfortunately, as the Killing field k^μ becomes space-like inside the black hole, the symmetrizer is not positive definite in this region.

We combine the advantages of both formulations by choosing $u^\mu = (k^\mu - b^\mu)/\alpha$, where b^μ is a smooth vector field which is tangential to the $t =$ const. slices, vanishes in a neighborhood of the outer boundary, and agrees with the shift vector β^i as one approaches the event horizon from the outside region. This new interpolating formulation is manifestly symmetric hyperbolic also inside the black hole; and at the outer boundary radiative boundary conditions can be given. Equations (6) yield

$$\begin{aligned}
\partial_t \Pi &= b^i \partial_i \Pi + \frac{\Delta^i}{\alpha} \partial_i (\alpha \Pi) + \frac{1}{\sqrt{h}} \partial_i (\sqrt{h} \Delta^i \Pi) \\
&+ \frac{1}{\sqrt{h}} \partial_i \left(\alpha \sqrt{h} H^{ij} V_j \right) - \frac{1}{\sqrt{h}} \partial_j \left(\sqrt{h} \frac{b^j}{\alpha} \right) \Delta^i V_i \\
&+ \frac{1}{\alpha} \left(\beta^j \partial_j b^i - b^j \partial_j \beta^i \right) V_i + \frac{1}{\sqrt{h}} \partial_i (\sqrt{h} b^i) \Pi \qquad (7) \\
\partial_t V_i &= \partial_i (\alpha \Pi) + b^j \partial_j V_i + V_j \partial_i b^j \qquad (8)
\end{aligned}$$

where $\Delta^i = \beta^i - b^i$, $H^{ij} = h^{ij} - \Delta^i \Delta^j / \alpha^2$, and

h^{ij} denotes the inverse three metric. This system is symmetric hyperbolic with respect to the energy $\mathcal{E} = \frac{1}{2}\int_\Omega \alpha\left(\Pi^2 + H^{ij}V_iV_j\right)\sqrt{h}d^3x$. The change of $\mathcal{E}$ under the flow generated by (7,8) can be bounded as

$$\frac{d}{dt}\mathcal{E} \leq \int\limits_{OB} \frac{1}{4}\left(w_+^2 - w_-^2\right)\sqrt{h}d^2x + \int_\Omega F d^3x, \qquad (9)$$

where $w_\pm = \mu_\pm\Pi + \alpha H^{ij}n_iV_j$ are the characteristic variables which have nonzero speeds, $\mu_\pm = \pm\alpha + \beta^i n_i$, and n_i is the normal to the outer boundary, normalized such that $h^{ij}n_in_j = 1$. The expression F in Eq. (9) vanishes if $b^i = 0$. Then setting w_+ to zero guarantees that $\mathcal{E}$ will decrease when the wave reaches the boundary. In the previous estimate we have assumed that the excised cube is sufficiently small (side length smaller than $4\sqrt{3}M/9$) so that the inner boundary is purely outflow.

Equations (7)–(8) have been written such that the replacement ∂_i by D_i (only on the dynamical variables) automatically leads to a semi-discrete system with energy conservation in the case $b^i = 0$. The semidiscrete solution will not grow, even at fixed resolution.

The figures show the results of the numerical implementation of the techniques for the scalar wave example we discussed; we have chosen Kerr-Schild coordinates (we have checked that the case of Painlevé-Gullstrand coordinates behaves similarly and so does the Maxwell field on these backgrounds) . Figure 1 shows evolutions with the computational domain outside the event horizon; fig. 2 shows results of a run with singularity excision. Movies can be see in [7].

In this article we have shown that the use of rigorous numerical analysis techniques can be used in practice to obtain stable schemes for numerical relativity. This maps out a precise road for robust implementations, reducing the need for expensive trial and error standard methods. The successful application of these techniques to the simulation of fields propagating on black hole backgrounds, which requires dealing with singularity excision, corners and edges, illustrates the potential of the approach. This opens the door for applying the same techniques to the full equations of general relativity.

Acknowledgments: We thank E. Tadmor, P. Olsson, and H. O. Kreiss for helpful discussions. This work was supported in part by NSF grant PHY9800973, the Horace Hearne Jr. Institute for Theoretical Physics, and Fundación Antorchas. Computations were done at LSU's Center for Applied Information Technology and Learning and parallelized with the CACTUS toolkit [8]. GC, LL, OR, OS and MT thank the Caltech Visitors Program in numerical relativity for hospitality.

[1] M. Alcubierre and B. Brugmann, Phys. Rev. D **63**, 104006 (2001); L. Kidder, M. Scheel, and S. Teukolsky, Phys. Rev. D **64**, 064017 (2001); H-J. Yo, T. Baumgarte, and S. Shapiro, Phys.Rev. D **64**, 124011 (2001); D. Shoemaker et. al, gr-qc/0301111.

[2] B. Gustaffsson, H.O. Kreiss, J. Oliger, *Time dependent problems and difference methods* (Wiley, New York, 1995).

[3] P. Secchi, Diff. Int. Eq. **9**, 671 (1996); Arch. Rat. Mech. Anal. **134**, 595 (1996).

[4] B. Gustaffsson, Math. Comp. **29**, 396 (1975); SIAM. J. Num. Anal. **18**, 179 (1981).

[5] P. Olsson, Math. Comp. **64**, 1035 (1995); **64**, S23 (1995);**64**, 1473 (1995).

[6] H.O. Kreiss and G. Scherer, SIAM J. Num. Anal. **29**, 640 (1992); H. O. Kreiss and L. Wu, Appl. Num. Math. **12**, 213 (1993); D. Levy and E. Tadmor, SIAM Rev. **40**, 40 (1998); E. Tadmor, Proceedings in Appl. Math. **109**, 25 (2002).

[7] http://relativity.phys.lsu.edu/movies/scalarfield

[8] http://www.cactuscode.org